Effects of Vibration Blending on the Subsequent Crystallization Behavior of Polycarbonate/Polypropylene Blends

KEJIAN WANG,* CHIXING ZHOU, WEI YU

Department of Polymer Science and Engineering, Shanghai Jiao Tong University, Shanghai 200240, China

Received 29 March 2001; accepted 6 August 2001

ABSTRACT: The effects of blending in a novel vibration internal mixer on the subsequent multiple crystallization of 70/30 w/w polycarbonate (PC)/polypropylene (PP) were investigated by differential scanning calorimetry, wide-angle X-ray diffractogram, and microscopy. The vibration internal mixer was reformed from a conventional internal mixer through parallel superposition of an oscillatory shear on a steady shear. For this polypropylene–minor phase blend, three possible crystallization peaks were observed. The crystallization behavior was sensitive to the sizes and the size distribution of the dispersed polypropylene droplets. Larger amplitude and/or higher-frequency vibration produced more small droplets (<2 μm) and increased the number of medium droplets (2–8 μm) as a result of the spatially wider and temporally quicker variation of shear rate. The resulting subsequent low-temperature crystallization peak became larger and shifted to lower temperature, and the intermediate-temperature peak became obvious. On the contrary, the coalescence of small droplets, resulting from the heating treatment, weakened the low-temperature peak but strengthened the intermediate-temperature peak and rendered the high-temperature peak to be wider. Mixing at the too high amplitude produced the unstable, partially cocontinuous phase morphology restricting the medium droplets and enlarging the surface area, such that the intermediate-temperature crystallization peak did not appear. Multiple crystallization was related to phase morphology and the nucleation density as well as surface effects. Double-fusion endotherms of the PP component were also observed, corresponding to the melting of different forms of polypropylene crystals. © 2002 Wiley Periodicals, Inc. J Appl Polym Sci 85: 92–103, 2002

Key words: polycarbonate/polypropylene; multiple crystallization; phase morphology; vibration; internal mixer

INTRODUCTION

The melting and cooling behaviors of polymers have been the subject of extensive investigation. Crystallizable polymers are generally nucleated by heterogeneities, effectively to induce crystallization at a specific undercooling. In fact, multiple crystallization behaviors were found in copolymers,[1,2] in which it was found that the crystallite grew parallel to the domain interface and crystallization drove microphase separation. Later, this phenomenon was also observed in immiscible polymer blends having a crystallizable minor phase.[3–5] With the practical and theoretical backgrounds, the multiple crystallization of polymer

**Present address:* National Engineering Research Center of Novel Equipment for Polymer Processing, China.

Correspondence to: C. Zhou (cxzhou@mail.sjtu.edu.cn).

Contract grant sponsor: National Nature Science Fund of China; contract grant number: 29634030-2.

Journal of Applied Polymer Science, Vol. 85, 92–103 (2002)

blends has been further investigated by some research groups.[6–18] It becomes clear that when a crystallizable polymer is finely dispersed in an immiscible noncrystallizable matrix, only a fraction of polymer droplets will contain active heterogeneities capable of nucleating the polymer at high temperatures. The rest of the droplets will need higher undercooling to activate other types of less-sufficient heterogeneities, and crystallize in one or more stages and/or eventually in homogeneous mode in the droplets, which lack active heterogeneous nuclei.[17] This phenomenon is called fractionated or multiple crystallization.[5–18] There are a limited number of reports about the fractionated crystallization in polymer blend systems reviewed in Everaet et al.[5]

The semicrystalline polypropylene (PP), from the commercial standpoint, is of prime importance, offering a combination of inexpensive price and easy processability.[19] However, PP has poor impact resistance at low temperatures. To improve the impact properties, it has been modified by other plastics. Its multiple crystallization in the blends was also observed in PP/thermoplastic rubber,[15] PP/polyamide-6,[13,20] PP/linear low-density polyethylene,[21] PP/polystyrene,[18] and PP/polycarbonate (PC).[22] Chun et al.[22] reported that two separate crystallization peaks of PP/PC blends with the minor phase of PP, as described by DSC, were attributable to different nucleation mechanisms. The low-temperature peak at about 85°C (homogeneous nucleation) was enhanced with increasing composition of PC, whereas the high-temperature peak at about 105°C (heterogeneous nucleation) decreased. Recently, the present authors used engineering plastics PC to toughen PP. During the course of the investigation, the low-temperature peak in the thermogram was not observed, whereas the other novel higher temperature crystallization peaks were found for 30/70 PP/PC prepared in a vibration field, in which their intensities and temperature positions varied for the samples mixed at the different conditions. These are reviewed in detail in this study.

The multiple steps of primary nucleation of the dispersed phase were not only related to phase morphology and nucleation density of the minor phase[5–17] but also influenced by blend type,[17] thermal history,[17] and previous mixing variables. For the PC/PP blends under consideration, PP is immiscible with PC[19]; therefore distinct methods of preparation could produce different morphologies and, thus, different crystallizations as well as product properties.[23] For instance, Yu and Choi[24] found that PP/thermoplastic rubber exhibited two low-temperature crystallization exotherms at 75°C and 45°C, in addition to the exotherm at 106°C, when the blend was made at the higher speed in the mixer. Morales et al.[21] observed that the presence of the left-oriented kneading screw blocks as well as the right-oriented kneading blocks in the twin-screw extruder increased the pressure gradient, leading to the reduction in particle size to 0.9 μm. As a result, stronger homogeneous nucleation in these particles occurred. It was recently found that vibration blending could also affect phase morphology,[25,26] and thus vibration blending could influence the subsequent crystallization. In this investigation, effort has been undertaken to study the effects of vibration conditions in mixing on the subsequent crystallization of PP in PP/PC blends using differential scanning calorimetry and microscopy techniques.

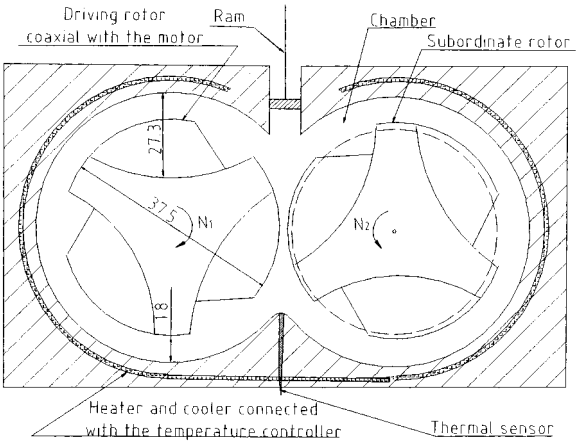

Figure 1 Schematic illustration of the vibration internal mixer.

EXPERIMENTAL

Vibration Internal Mixer

A used vibration internal mixer was reformed from a conventional batch internal mixer, as shown in Figure 1, by forcing just two rotors to oscillate in the revolution, as illustrated in Figure 2. The rotors are mounted on parallel shafts and rotate in the opposite directions. The driving rotor gears the subordinate rotor, in which their transient speed ratio is kept at 3 : 2, and the shaft of the driving rotor is driven by a motor controlled by a vibrator. The maximum diameter of the two

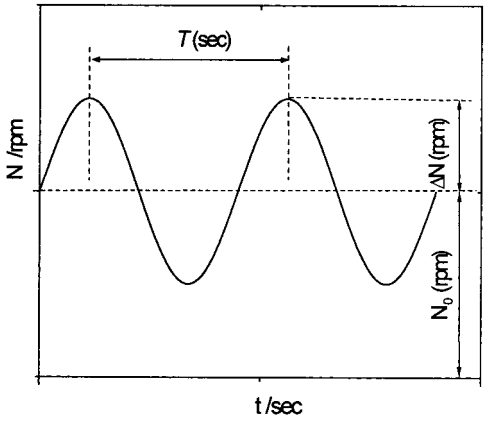

Figure 2 Diagram of the oscillatory function of rotor speed.

rotors is 37.5 mm, and the gap (δ) between the rotors and the chamber ranges from 1.8 to 27.3 mm.

The speed of the driving rotor can be written according to the superposition of an oscillatory speed on the steady speed as $N(t) = N_0 + (\Delta N)F(t)$, displayed in Figure 2. Here t (s) is time, N_0 (rpm) is the steady average speed reached in a short startup by the driving rotor, and ΔN (rpm) is its vibration amplitude. Here, $F(t)$ is the controllable harmonic function, expressed as $F(t) = \sin(2f\pi t)$, with vibration frequency f (Hz) (equal to the inverse of the vibration period T in Fig. 2). These vibration parameters and the mixing temperature are preset before compounding or plasticizing the polymers. For simplicity, the conditions for blending or plasticizing in the vibration internal mixer can be denoted, by convention, as vibration mode *Vib–*N_0*–* ΔN*–* f in this context. Blending or plasticizing at a constant N with $\Delta N = 0$ is the conventional steady mode *Steady–N*. For instance, the symbol *Vib 50–10–0.5* indicates a vibration running with $N_0 = 50$ rpm, $\Delta N = 10$ rpm, and $f = 0.5$ Hz; and *Steady 50* means a steady running at $N = 50$ rpm. The steady mode could be regarded as a special vibration mode with zero amplitude or with zero frequency.

Materials and Sample Preparations

Granular polycarbonate of 2,2-bis(4′-hydroxyphenyl)propane (PC; trademark T100) with T_g of 146°C was obtained from Sanyang Chemical Co. (China). An isotactic polypropylene (PP; trademark PP 1647c), in granular form, was manufactured by Yanshan Petrochemical Co. (Beijing, China).

All original materials were dried under vacuum at 100°C for 24 h before use. A 45-g sample of PC/PP was dry mixed at room temperature in a fixed-weight composition 70/30 PC/PP and then blended in the vibration internal mixer at 220°C with the designed parameters. After blending, the samples were quenched to room temperature. It should be noted that some of the pure PP was also plasticized at 220°C under the same conditions for comparison. Some slices were compressed from each sample, which was taken from the mixer chamber after blending for 15 min.

Tests

The PC in the blend slices was dissolved by trichloromethane for phase morphology analysis by a scanning electron microscope (SEM S-2150; Hitachi Co., Japan) after gold sputter-coating.

The plasticized pure PP in steady shear was compression-molded at 30°C and under elevated pressure up to 30 MPa for 3 min so as to obtain a 0.3- to 0.5-mm-thick film for wide-angle X-ray diffraction (WAXD) analysis. WAXD measurement was conducted at 35 kV and 25 mA using Ni-filtered CuK_α radiation on a diffractometer (D/MAX-III; Rigaku, Tokyo, Japan).

The melting and crystallization behaviors of the pure PP, PC, and PC/PP blends were studied by a differential scanning calorimeter (PYRIS DSC-7; Perkin Elmer Cetus Instruments, Norwalk, CT). The samples were heated quickly to 220°C and kept at 220°C for 5 min to eliminate the previous thermal history. After that, it was cooled to 50°C at 10°C/min and then heated back to 220°C at 10°C/min. To make certain that the thermal lag between the polymer sample and the DSC sensors was kept to a minimum, each sample was weighed ($\sim 5.8 \pm 0.3$ mg) and used only once. Temperature calibration was performed using an indium standard and all the runs were performed under a nitrogen purge.

The evolutions in the phase morphologies of PP and PC/PP were analyzed by a polarized-light microscope equipped with a hot stage (model Steren Scan 440; Leica, Wetzlar, Germany). Some samples were heated to 250°C and then cooled to room temperature at 10°C/min to observe the sequence of crystallization in droplets with different sizes. The other samples were also heated quickly to 250°C and held for 5–10 min or heated up to 280°C and held for 10 min to record the changes in morphology during annealing. After the optical observation, each sample was immediately quenched to room

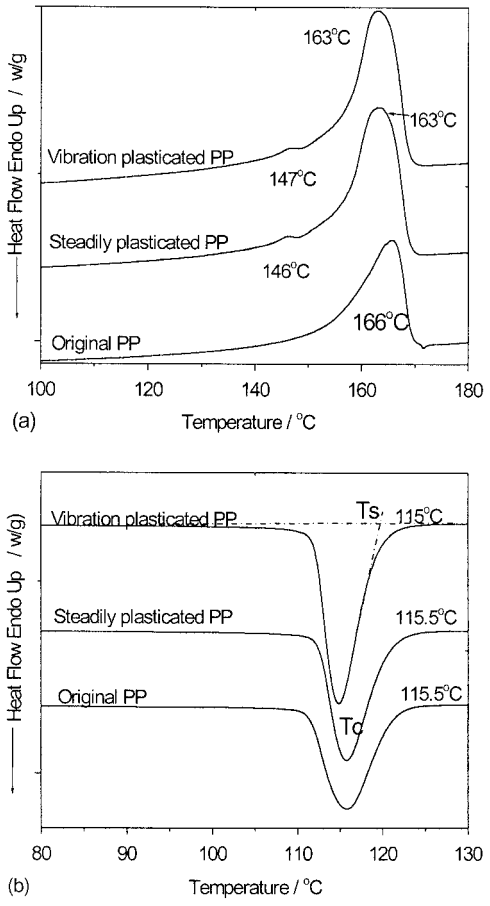

Figure 3 DSC melting thermograms (a) and crystallization thermograms (b) of the original PP, the vibration-plasticized PP, and the steadily plasticized PP.

temperature at 30°C/min. Each quenched sample was further tested by DSC, in which the running was the same as the foregoing.

RESULTS AND DISCUSSION

Melting and Crystallization of PP

DSC thermograms of PP treated under different conditions are shown in Figure 3. In the fusion endotherms of Figure 3(a), the original PP exhibits only a single melting peak at 166°C, but the plasticized PP shows double peaks. The lower peak at about 146°C corresponds to the melting of the hexagonal β-form crystal of PP, which subsequently recrystallized into the monoclinic α-form whose peak lies at 163°C. Similar cases were found in research by Bousmina et al.[27] and Turner-Jones et al.[28] For the PP plasticized in the vibration mode (vibration plasticization), the lower-temperature melting peak changed from 146 to 147°C of PP plasticized in the steady mode (steady plasticization), whereas the higher-temperature peak remained constant.

From the respective DSC fusion peaks in Figure 3(a), the degree of crystallinity of α-PP and β-PP could be calculated according to

$$\Phi_i = \frac{\Delta H_i}{\Delta H_i^\circ} \times 100\% \qquad (1)$$

where ΔH_i is the fusion heat of either α-PP or β-PP from the DSC thermogram and ΔH_i° is the standard fusion heat, which is 170 and 178 J/g for α-PP and β-PP, respectively.[28] The calculated results are listed in Table I. The original PP has the lowest crystallinity, whereas the previous plasticization increases the crystallinity of either α-PP or β-PP. The crystallinity of the β-form in the vibration-plasticized PP is slightly higher than that of the steadily plasticized PP.

Figure 3(b) illustrates the effects of previous plasticization on the crystallization, from which the onset crystallization temperature T_s, the crystallization peak temperature T_c, and the slope F (w g^{-1} K^{-1}) of the slantwise line at the higher-temperature side are calculated and given in Table I. It is found that steady plasticization has scarcely any effect on T_s and T_c, whereas vibration plasticization decreases both variables, forming narrower values of ($T_s - T_c$) and the highest value of F. Supaphol[29] used a time t_c to denote the time that the sample spent from the melt state to

Table I Crystallization Parameters of PP Prepared Under Different Conditions

Material	ϕ_β (%)	ϕ_α (%)	T_s (°C)	T_c (°C)	$T_s - T_c$ (°C)	F (w g^{-1} K^{-1})	ΔH_c (J/g)
Original PP	0	36.4	122	116	6	37.8	73
Steady PP[a]	0.15	36.8	122	116	6	45.7	79
Vib-PP[b]	0.20	36.6	120	115	5	50.9	93

[a] PP plasticated in steady mode.
[b] PP plasticated in vibration mode.

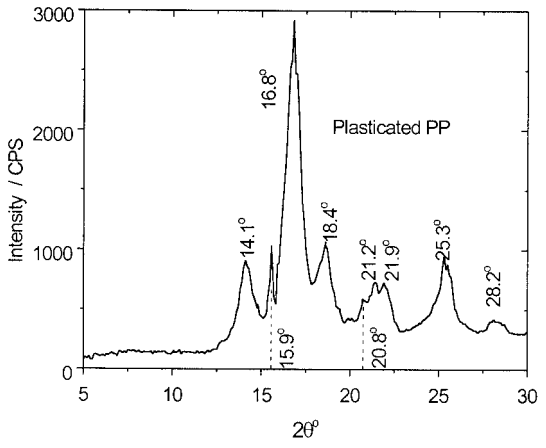

Figure 4 Wide-angle X-ray diffractogram of the plasticized PP.

the peak temperature T_c with a maximum crystallization rate for syndiotactic polypropylene. The reciprocal value of t_c could describe the rate of nonisothermal crystallization. At the same constant cooling rate for our three samples, t_c^{-1} is proportional to $(T_s - T_c)^{-1}$, capable of indicating the crystallization rate. Likewise, the crystal growth rate is inversely related to $(T_s - T_c)$. F is proportional to the nucleation rate. The higher nucleation rate confirms the increased amount of heterogeneity after vibration plasticization. The higher nucleation rate contributes to the higher crystallinity together with quicker crystallization.

The existence of the β-form crystal of PP in the plasticized samples must be substantiated by WAXD and polarized optical microscopy. In WAXD patterns, as illustrated in Figure 4, the α-form crystal is overwhelmingly prevalent, with the following X-ray reflections ($2\theta_{Cu}$): 14.1° (110), 16.8° (040), 18.4° (130), 21.2° (111), 21.9° (131), and 25.3° (041). However, as indicated by the dotted line at the $2\theta_{Cu}$ reflections of 15.9° (300) and 20.8° (301), the hexagonal β-unit cell structure is also included in the sample, although its relative content is low. From the respective WAXD patterns, the relative amount of β-phase with respect to α-phase is about 5%, which is close to the value calculated from their crystallinity, as implied in Table I. In addition, the wide ridgelike spandrel under the peaks is obvious as a consequence of quenching the sample to room temperatures, which thus led to a phase of intermediate order between the amorphous phase and the crystalline phase. Thereby, different processing conditions could generate different degrees of stereoirregularity; the plasticized sample is phase-mixed.

It is known that the flowerlike β-form polypropylene spherulites with lamella petals continuously branch into twisted arcs, thus causing the brilliantly colored interferential patterns in polarized-light microscopy that can be used to distinguish the β-form from the α-form.[30,31] It is observed that the scattered small colorful spherulites indeed appeared among the numerous large spherulites in crystallization of the plasticized PP. This proves the existence of β-form crystals among the α-form crystals, that is, the low-temperature fusion peak is attributed to the β-form crystal. As is known, the α-form crystallite is by far the most common in most melt-crystallized PP samples. The metastable β-modification appears under special crystallization conditions such as in the sheared melt of PP.[32–34] Karger-Kocsis[35] found that melt shearing, caused by fiber pulling, was associated with the development of α-row nuclei, whose surface induced the growth of the β-form of PP. In the vibration internal mixer, the shear rate varies both spatially and temporally. The complex shear gradient field possibly increases the amount of β-PP in the subsequent crystallization.[23] The β-form crystal recrystallized and reorganized into the α-form by melting at 150°C.[27,28] The twin melting peaks are of different crystal forms with different degrees of perfection caused by the thermal history (such as plasticization).[30]

Effects of Vibration Blending on the Subsequent Multiple Crystallization of PC/PP

In the DSC fusion thermogram, as shown in Figure 5, PP/PC exhibits two peaks like those of the plasticized pure PP, which correspond to the melting of β-PP and α-PP, respectively. They shift to slightly lower temperatures compared with those of the plasticized pure PP. In fact, the glass transition of PC at 146°C is overlapped by the melting peak of β-PP.

The single crystallization peak of PP turns double after vibration blending with PC in the Vib 50–20–0.25 mode, as shown in Figure 5. The high-temperature crystallization peak lies at 116°C, whereas the low-temperature peak is at 100°C. The almost consistent melting behaviors of PP and PP/PC exclude the change of crystal lamellar texture as the dominant origin for the multiple crystallization peaks of PC/PP; rather, as detailed in the next section, the subsequent

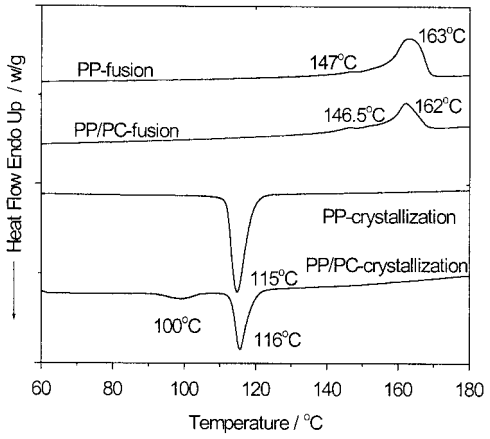

Figure 5 DSC thermograms of PP and PC/PP prepared in the Vib 50–20–0.25 mode.

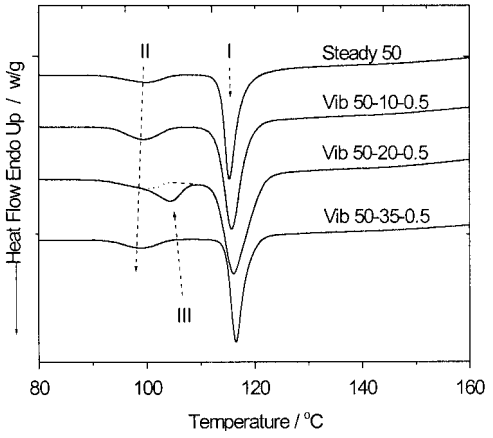

Figure 7 DSC crystallization thermograms of PC/PP blended in steady mode or in vibration mode with the different vibration amplitudes at the fixed N_0 = 50 rpm and f = 0.5 Hz.

steps of primary nucleation of the dispersed phase PP are responsible for it.[5,22] In the following, the influences of the mixing conditions on crystallization of PC/PP are discussed further.

The cooling curves of 70/30 PC/PP blends prepared at different frequency vibrations at the fixed N_0 = 50 rpm and ΔN = 20 rpm are displayed in Figure 6. For the samples steadily mixed or vibration blended at f = 0.25 Hz, peak I at about 115°C and peak II at about 100°C are observed. For samples made at higher-frequency vibrations (such as f values of 0.5 and 1.0 Hz), another novel peak III at about 104°C is observed overlapped partly with peak I and connects with peak II. Moreover, peak II shifts to the lower temperature and its area becomes larger in the blends prepared in the higher-frequency vibrations. On the contrary, peak I becomes wider. In addition, peak III shifts slightly to a higher temperature with a larger area.

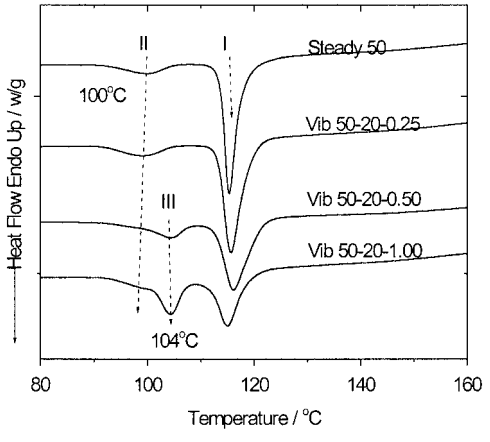

Figure 6 DSC crystallization thermograms of PC/PP blended in steady mode or in vibration mode with the different frequencies at the fixed N_0 = 50 rpm and ΔN = 20 rpm.

The influences of the different amplitude vibrations on the subsequent crystallization are illustrated in Figure 7. The high-temperature crystallization peak I shifts to higher temperature, and its initial crystallization temperature also shifts upward with a wider crystallization temperature range for the samples made at the increased vibration amplitude at the same N_0 = 50 rpm and f = 0.5 Hz, except the case at ΔN = 35 rpm. The peak at about 100°C becomes more obvious; in particular, the peak at about 104°C appeared in the sample made at ΔN = 20 rpm, although it did not appear at a higher amplitude such as that at ΔN = 35 rpm. This abnormality is related to the difference in morphology of the sample, as discussed below.

Analyses by Combined DSC and Optical Microscopy

To examine whether there are some correlations between the multiple crystallization behaviors and the phase morphology (i.e., cocontinuous or discrete dispersed droplets/matrix, their sizes, and their size distributions), the more direct experiments were carried out by annealing the sample on the hot stage placed under an optical microscope, and the resultant samples with specifically observed phase structures were quickly frozen and analyzed by DSC.

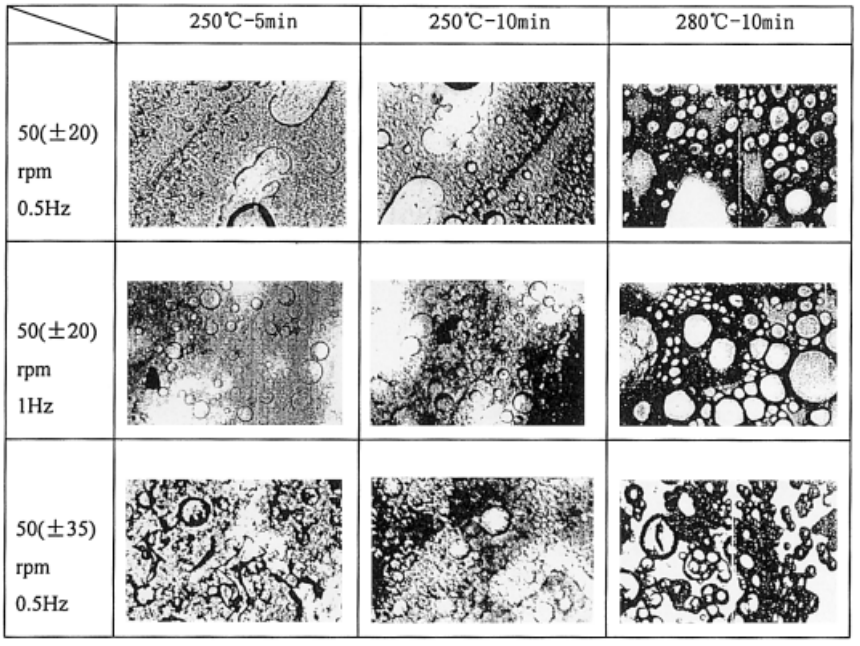

Figure 8 Polarized light micrographs of the 70/30 PC/PP blends prepared in the different modes with coalescence of smaller droplets.

First, a test was performed to observe the sequence of crystallization in droplets of different sizes. The blend samples were quickly heated to 250°C and then cooled to room temperature on the hot stage. Dark points were found to appear at about 130°C in large polypropylene droplets (>8 μm), and the visual field became semitransparent. When cooled to 115°C, the formed grains grew quickly into large spherulites. When the temperature dropped to about 110°C, intermediate droplets began to crystallize. The drastic increase in the number of tiny crystals was instantaneously observed at about 95°C, which means that crystallization in tiny droplets (<2 μm) occurred instantaneously. Furthermore, most crystals were colorless with a few sporadic coloring sprinkles, indicating that α-form crystals are predominant with a small amount of β-form crystals.

Second, analyses by DSC and optical microscopy were combined to explore the relationship between the multiple crystallization and the phase morphology. Figure 8 shows the morphology evolutions of PC/PP blended in the Vib 50–20–0.5 mode, the Vib 50–20–1.0 mode, and the Vib 50–35–0.5 mode. The number of medium-size droplets in the sample prepared in either the Vib 50–20–1 mode or the Vib 50–35–0.5 mode is greater than that in the Vib 50–20–0.5 mode. Upon being heated to 250°C for 5 min, the solid blend melted and became increasingly transparent; PP droplets in the PC matrix melted, although the phase morphology was maintained because PC cannot flow at first. Further isothermal heating can induce the softened PC to flow because of the preserved compression in the previously prepared sample between two thin glass plates, thus causing the PP droplets to deform or even to coalesce. To quicken coalescence, we elevated the temperature to 280°C, maintained for 10 min. Under such a condition, the size of droplets increased and the initial tiny particles cannot be observed. The number of small droplets decreased, whereas the number of the medium- or large-size droplets increased. In the PC/PP sample made at the Vib 50–35–0.5 mode, the observed irregular domains retracted into ellipsoids and further into spheres when heated for 10 min at 250°C, that is, the metastable and partly cocontinuous phase morphology transformed into the completely dispersed phase.

After the optical observations, the frozen samples were dried under vacuum and then examined by DSC. Their cooling curves are given in Figure 9. In Figure 9(a) for the samples mixed at higher frequencies, three peaks all appear. When the sample was heated to 250°C and held for 10 min or heated at 280°C for 10 min, coalescence occurred, as illustrated in Figure 8. The correspond-

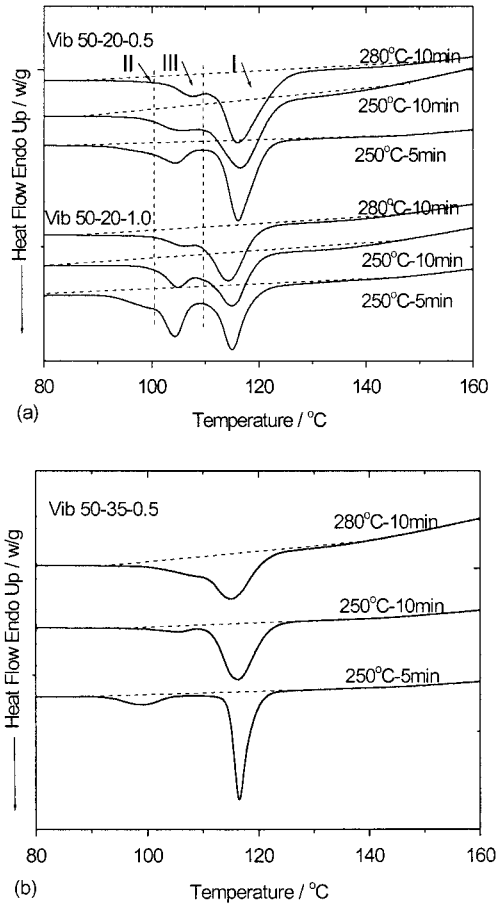

Figure 9 The changes in DSC crystallization thermograms of 70/30 PC/PP blended at different frequency vibrations (a) at the fixed $\Delta N = 20$ rpm and in the Vib 50–35–0.5 mode, and (b) after coalescence of smaller droplets.

ing DSC peak I widens, and the transition between the peaks occurs gradually. The area of peak II decreases, whereas the area of peak III becomes larger. Thereafter, variations in the thermograms are assumed to be attributed to the changes in the sizes of dispersed droplets of PP as well as their size distribution. Peak I mainly reflects the crystallization of PP in large droplets, whereas peak III should be associated with the crystallization of PP in the intermediate droplets. The decline in the area of peak II is indicative of the decreasing number of small particles. Their coalescence leads to more intermediate droplets, corresponding to a wider peak III connecting with peak I for the heated sample. In Figure 9(b), the sample made in the Vib 50–35–0.5 mode first exhibits two separate peaks. When the sample is heated for 10 min at 250°C, as shown in Figure 8, the unstable cocontinuous phase structure transforms into the completely dispersed phase structure. Subsequently, peak I in the DSC exotherm is widened; the low-temperature peak shifts to higher temperature at 105°C as a peak III and links with peak I. For the sample heated at 280°C, peak I becomes wider and the area of peak III is relatively larger. The latter case tells us that the effects of medium-size droplets increase. The appearance of peak III shows that the phase type affects the crystallization.

Phase Morphology of PC/PP Blends

In vibration blending, the strong shear occurs in the gaps between the rotors and chamber wall. The shear rate on the surface of the driving rotor could simply be expressed as

$$\dot{\gamma} = \pi DN/\delta = \pi D[N_0 + \Delta N \sin(2\pi ft)]/\delta \quad (2)$$

where D is the specific diameter of the rotor surface. It is found from eq. (2) that $\dot{\gamma}$ changes with D and t. In one period, $\dot{\gamma}_{\min}$ occurs at the minimum diameter and $N = N_0 - \Delta N$, whereas $\dot{\gamma}_{\max}$ at the maximum diameter and $N = N_0 + \Delta N$. In a steady mode at $N = 50$ rpm, $\dot{\gamma}$ ranges between 1.15 and 54.7 s^{-1}; in a vibration mode with $N_0 = 50$ rpm and $\Delta N = 35$ rpm, $\dot{\gamma}$ ranges between 0.35 and 93 s^{-1}. Similarly, the transient shear rate at the subordinate rotor could also be obtained by replacing N with its speed of rotation into eq. (2). Accordingly, the range of shear rate widens with ΔN, and f shows such variation rhythm. The larger amplitude and/or higher frequency vibration blending could influence the processes of the droplet breakup and coalescence. Specifically, it reduces the average droplet size and widens the size distribution of the medium droplets.

In our previous study,[25] it was found that the same 30/70 PP/PC blends mixed in vibration mode exhibited lower shear viscosity than those mixed in the steady mode. In samples prepared with larger ΔN or higher f values, such a drop in the shear viscosity was more significant, except that the blend mixed in the Vib 50–35–0.5 mode was more viscous than the blend prepared in the Vib 50–20–0.5 mode. The latter exception was related to the preceding complex morphology. The flow temperature for PC, approximately 55°C above its T_g of 146°C, was higher than the bulk $T_m = 163$°C of PP.[36–38] The melted PP tended to encapsulate the softened PC in the initial blending. The continuous mixing eased the flow of PC,

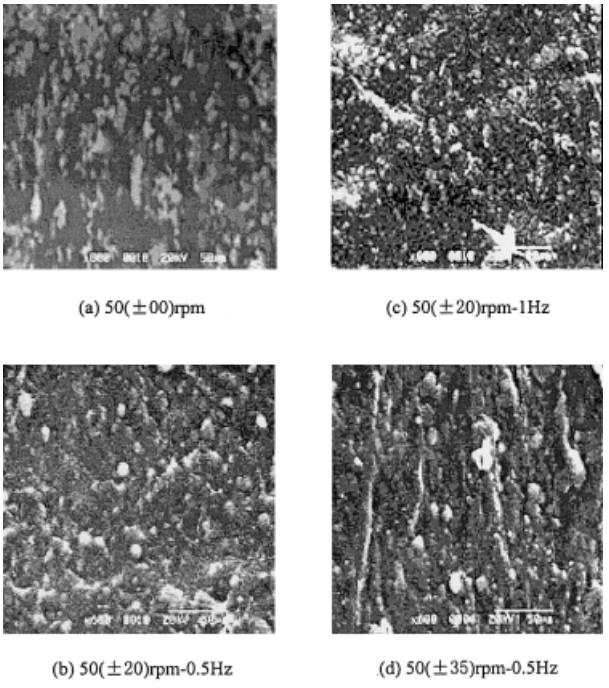

Figure 10 SEM micrographs showing the distribution of the droplets in 70/30 PC/PP blends prepared in different modes. Bar: 50 μm.

such that PP was more prone to shear thinning than was PC.[25] Equation (2) shows that the vibration with very large ΔN enhances the probability that, at very low or very high shear rates, the viscosity ratio of two components will frequently alternate. Thus, the phase inversion is possibly delayed, which may cause the partially continuous phase morphology in the Vib 50–35–0.5 mode.

The micrographs, presented in Figure 10(a)–(c) and Figure 11(a)–(c), show that the minor-phase PP formed the dispersed droplets. The middle-scale and large-scale droplets are evident in Figure 10, in which the number of small droplets becomes greater in the samples that were vibration blended than those in the steadily blended sample, and vibrations with larger f or ΔN values really promote such effects to a higher degree. In Figure 11, obtained with greater optical magnitude, PP droplets overlap because of the overdissolution of the matrix PC. The diameter of small droplets is less than 2 μm, large droplets are greater than 8 μm, and the number of droplets with intermediate diameters (2–8 μm) is greater in the higher f or larger ΔN vibrations. Furthermore, there seem to be residues of the partially cocontinuous unstable phase structure for the blend mixed in the Vib 50–35–0.5 mode, as shown in Figures 10(d) and 11(d). When it was heated to 280°C, large stream domains disappeared, as shown in Figure 8.

Correlative Factors of Multiple Crystallization Behavior

All primary nucleations in polymer crystallization can be classified into three types: homogeneous, heterogeneous, and self-seeding. Homogeneous nucleation is sporadic with constant rate and is dependent on the temperature of crystallization, whereas at low or intermediate undercooling, heterogeneous and self-seeding nucleations are frequently observed with some induction time.[39] Despite the different material characteristics, the wide size distribution of spherulites of dispersed PP could disturb the nucleation, or vice versa.[7,16,40] The crystallization of the dispersed small droplets crucially depends on their sizes because of the distribution of heterogeneous nuclei[12] and their broad spectrum of activity.[10] Some nuclei are highly active and able to cause instantaneous nucleation of iPP at higher crystallization temperatures, whereas the less-active nuclei appear to crystallize spontaneously at a lower temperature.[10] In our experiment, higher-frequency or larger-amplitude vibration produces

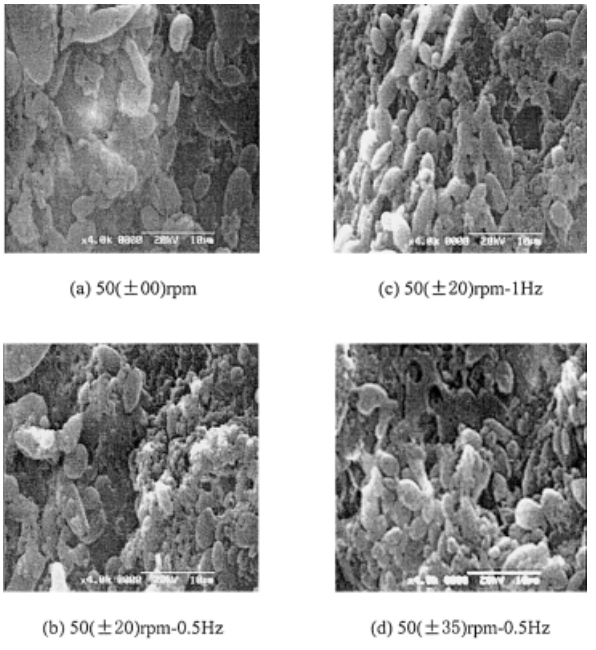

Figure 11 SEM micrographs showing the sizes of the droplets in 70/30 PC/PP blends prepared in different modes. Bar: 10 μm.

a greater number of smaller droplets. It is widely accepted that homogeneous nucleation of PP occurs at about 80°C,[22,24] which is significantly lower than the nearly 100°C of peak II in Figures 7 and 9. Therefore, we expect that all three peaks in Figures 6 and 7 are caused by heterogeneous nucleation: crystallization in large droplets corresponds to peak I and the crystallization in small droplets corresponds to peak II, whereas some droplets of intermediate sizes created under the appropriate vibration conditions may possibly lead to the occurrence of peak III. A larger peak III indicates a rather sizable amount of medium-size droplets; the shift of peak II to a slightly lower temperature is attributed to more tiny PP droplets.[22,24,41]

Heterogeneous crystallization occurs only in a volume containing at least one active heterogeneity at a certain temperature.[42,43] Generally, potential heterogeneous nuclei for PP include foreign impurities, catalyst residues, amorphous PP phase, and unmelted tiny PP crystals. The volume nucleation density and the interface effect substantively play important roles in the primary nucleation. According to Frensch's theory,[42] crystallization occurring at high undercooling is generated from heterogeneities with large specific interfacial energy difference $\Delta\nu$ between the polymer chain and the nucleating substrate. Large droplets with the predetermined active heterogeneities, whose $\Delta\nu$ is smallest, can crystallize efficiently and spread over the whole volume at low supercooling. Some of the intermediate droplets do not have sufficient primary nuclei of critical size at a high temperature. The smaller or less-perfect heterogeneities can grow to the critical size, that is, the nucleation is sporadic at higher undercooling. Some of impurities on the surfaces of droplets are engulfed during droplet coalescence. They act as the heterogeneities in the subsequent crystallization, which reduces the free energy of action for primary nucleation and renders the formed larger droplets to crystallize at higher temperature.

Additionally, crystallization could occur at the surface of the intermediate droplets with a relatively lesser amount of heterogeneities within, although the resultant crystal growth rate is slow.[41,44,45] As the droplets become too small, volume limitation will significantly slow down the crystallization kinetics, forcing small droplets to crystallize at much higher undercooling.[46] Chipra et al.[47] found that the ratio of the internal energy of the system versus the interfacial area, that is, a dynamic interfacial tension Γ, varied with shear rate in the transient flow for 50/50 poly(styrene-*co*-maleic anhydride)/poly(methyl methacrylate), although Γ approached its static equilibrium value in the limit of zero-shear rate. The ratio of Γ to the average droplet diameter increased with increasing shear rate or with dropping the mixing temperature from 230 to 225°C. We also found an analogous situation for 70/30 PC/PP in vibration blending.[25] Therefore, the interfacial energy changes with flow and thus with surface curvature.[47] Vibration improves the penetration of one component into the other, thus obscuring, as it were, the phase interface.[48] Heterogeneities could exist on the interface and the aggregates of the polycarbonate phase could also act as nuclei.[49] The interface-induced additional nonhomogeneous nucleation could, equivalently, increase the number of the active heterogeneities.[41,44,45] This case is significant in the samples made at larger f or ΔN, which partially explains the appearance of peak III at 105°C. The interface-induced heterogeneous nucleation is significantly enhanced when the partially continuous phase morphology with too large an interface area is formed in the sample made in the Vib 50–35–0.5 mode. This induces the crystallization at low undercooling, corresponding to the upward shift of peak III to peak I, that is, peak III seems to disappear, as shown in Figure 9(b).

Thus, it can be seen that besides the thermodynamic factors such as temperature, pressure, and other annealing conditions, the rheological properties of the blends and the features of flow field in the previous mixing indirectly affect multiple crystallization because they influence the blend phase morphology.[24,42] Crystallization is sensitive to the thermal history, that is, crystallization has a memory effect.[50] From this point of view, crystallization could prospectively be used to analyze the phase-dispersion type[18,21] and the degree of dispersion (particle size)[15,46] when the minor phase exhibits multiple crystallization. The present focus has been directed toward the effects of vibration blending and the effects of annealing conditions on the subsequent crystallization of the 70/30 PC/PP blend.

CONCLUSIONS

Double-fusion endotherms were observed in a polypropylene after plasticization; the peak at about 163°C was of the α-form crystal in PP,

whereas the peak at about 146°C was that of the β-form. The presence of the latter crystal was confirmed by WAXD and polarized microscopy. Vibration blending could improve the dispersion of components in 70/30 PC/PP blends by reason of spatially wider and temporally quicker variation of shear rate in the vibration internal mixer. Vibration boosted the probabilities of droplet breakup and coalescence, which integratively produced more small particles (<2 μm) and increased the number of medium droplets (2–8 μm), thereafter transforming the subsequent single crystallization of pure PP into multiple crystallization of PC/PP.

The effects of vibration on the subsequent fractionated crystallization were complex. The typical homogeneous nucleation was absent, although some novel higher-temperature exotherms occurred. One crystallization was at about 100°C in the small polypropylene droplets, but the bulk crystallization was at about 115°C by predetermined heterogeneous nucleation in the large droplets (>8 μm). The former shifted to a relatively lower temperature, whereas the latter shifted to a higher temperature in samples prepared in the increased amplitude and/or frequency vibrations. More important, another novel intermediate-temperature crystallization peak was found in the medium droplets in the samples made in the higher frequency and/or larger amplitude vibrations. This peak embodied a larger number of the intermediate polypropylene droplets. Normally, vibration superposition increased the amount of small droplets and strengthened the intensity of the lowest-temperature crystallization, whereas the heating treatment caused droplets to coalesce and thus enhanced the intermediate-temperature crystallization. Generally, the minor phase of PP was dispersed as droplets, but too large amplitude vibration blending could induce a partially continuous phase morphology by the frequent alternation between low shear and high shear. The intermediate droplets became the subinclusions restricted by the large unstable continuous domains, which caused them to behave as large droplets in DSC, such that only low- and high-temperature crystallizations appeared. This partially continuous phase morphology transformed into the completely dispersed phase morphology when heated, and the intermediate-temperature crystallization peak appeared again.

The multiple steps of nucleation in the droplets with a wide size distribution were attributed to the distribution of the contained heterogeneities and the spectrum of their activity as well as the surface effects for the different size droplets. The multiple crystallization, related to the phase morphology and nucleation density of the minor phase, together with rheology may be prospectively used to analyze the phase morphology when the minor phase exhibits multiple crystallization.

The authors appreciate the financial support from the National Nature Science Fund of China (Grant 29634030-2). The authors also extend thanks to Professor Giovanni C. Alfonso for stimulating discussions.

REFERENCES

1. Malley, J. O. Crystal, Block Copolymers; Plenum: New York, 1970.
2. Rangarajan, P.; Register,R. A.; Fetters, L. J. Macromolecules 1993, 26, 4640.
3. Aref-Azar, A.; Hay, J. N. J Polym Sci Polym Phys Ed 1980, 18, 637.
4. Tang, T.; Huang, B. J Appl Polym Sci 1994, 53, 355.
5. Everaet, V.; Groeninckx, G.; Aerts, L. Polymer 2000, 41, 1409.
6. Arnal, M. L.; Müller, A. J. Macromol Chem Phys 1999, 200, 2559.
7. Arnal, M. L.; Balsamo, V.; Ronca, G.; Sanchez, A.; Müller, A. J.; Canizales de Navarro, E.; Urbina, C. J Therm Anal Calorim 2000, 59, 451.
8. Fillon, B.; Wittmann, J. C.; Lotz, B.; Thierry, A. J Polym Sci Part B: Polym Phys 1991, 31, 1383.
9. Blom, H. P.; Teh, J. W.; Rudin, A. Polymer 1998, 39, 4011.
10. Bartczak, A.; Pracella, M. J Appl Polym Sci 1994, 54, 1513.
11. Barham, P. J.; Jarvis, D. A.; Keller, A. J Polym Sci Polym Phys Ed 1982, 20, 1733.
12. Gornick, F.; Ross, G. S.; Frolen, L. J. J Polym Sci Polym Phys Ed 1967, 18, 70.
13. Ikkala, O. T.; Holsti-Miettinen, R. M.; Seppälä, J. J Appl Polym Sci 1993, 49, 1165.
14. Bogoevagaceva, G.; Janevski, A.; Grozdanov, A. J Appl Polym Sci 1998, 67, 395.
15. Ghijsels, A.; Groesbeek, N.; Yip, C. W. Polymer 1982, 23, 1913.
16. Galeski, B.; Piorkowska, E. J Polym Sci Polym Phys Ed 1980, 19, 731.
17. Manaure, A. C.; Morales, R. A.; Sanchez, J. J.; Müller, A. J. J Appl Polym Sci 1997, 66, 481.
18. Santana, O. O.; Müller, A. J. Polym Bull 1994, 32, 471.
19. Zhihui, Y.; Xiaomin, Z.; Yajie, Z.; Jinghua, Y. J Appl Polym Sci 1997, 63, 1857.
20. Moon, H. S.; Ryoo, B. K.; Park, J. K. J Polym Sci Polym Phys Ed 1994, B32, 1427.

21. Morales, R. A.; Arnal, M. L.; Müller, A. J. Polym Bull 1995, 35, 379.
22. Chun, Y. S.; Jung, H. C.; Han, M. S.; Kim, W. N. Polym Eng Sci 1999, 39, 2304.
23. Wang, K. J.; Zhou, C. X. Polym Eng Sci, to appear.
24. Yu, Y. S.; Choi, K. J. Polym Eng Sci 1997, 37, 91.
25. Wang, K. J.; Zhou, C. X. Polym Mater Sci Eng, to appear.
26. Tincer, T.; Coskun, M. Polym Eng Sci 1993, 33, 1243.
27. Bousmina, M.; Ait-Kadi, A.; Faisant, J. B. J Rheol 1999, 43, 415.
28. Turner-Jones, A.; Aizlewood, J. M.; Beckett, D. R. Macromol Chem 1964, 74, 134.
29. Supaphol, P. J Appl Polym Sci 2000, 78, 338.
30. Li, J. X.; Cheung, W. L.; Jia, D. M. Polymer 1999, 40, 1219.
31. Dong, Q. Z.; Guo, Q. Chin Synth Fiber Ind 1999, 22, 1.
32. Leugering, H. J.; Kirsch, G. Makromol Chem 1973, 33, 17.
33. Wu, C. M.; Chen, M.; József, K. K. Polym Bull 1998, 41, 493.
34. Jay, F.; Haudin, M. J.; Monasse, B. J Mater Sci 1999, 34, 2089.
35. Karger-Kocsis, J. Polym Eng Sci 1996, 36, 203.
36. Lee, J. K.; Han, C. D. Polymer 1999, 40, 6277.
37. Han, C. D.; Lee, J. K.; Wheeler, N. C. Polym Eng Sci 1996, 36, 1360.
38. Lee, J. K.; Han, C. D. Polymer 2000, 41, 1799.
39. Wunderlich, B. Macromolecular Physics: Crystal Nucleation, Growth, and Annealing, Vol. 2; Academic: New York, 1976.
40. Bartczak, Z.; Galeski, A.; Pracella, M. Polymer 1986, 27, 537.
41. Koutsky, J. A.; Walton, A. G.; Baer, E. J Appl Phys 1967, 38, 1832.
42. Frensch, H.; Jungnickel, B. J. Plast Rubber Compos Process Appl 1991, 16, 5.
43. Billon, N.; Haudin, J. M. J Therm Anal 1994, 42, 679.
44. Klemmer, N.; Jungnickel, B. J. Colloid Polym Sci 1984, 262, 381.
45. Burns, J. R.; Turnbull, S. J Appl Phys 1966, 37, 4021.
46. Billon, N.; Chanial, L.; Vivien, B.; Haudin, J. M. Colloid Polym Sci 1995, 20, 355.
47. Chopra, D.; Vlassopoulos, D.; Hatzikiriakos, S. G. J Rheol 2000, 44, 27.
48. Ibar, J. P. Polym Eng Sci 1998, 38, 1.
49. Silvestre, S.; Cimmino, E. D.; Alma, M. L.; Dilorenze, E. D. Polymer 1999, 40, 5119.
50. Alfonso, G.; Ziabicki, C. Colloid Polym Sci 1995, 273, 317.